Characterization of piezoelectric stacks for Space Applications

Stewart Sherrit, Christopher Jones, Jack Aldrich, Chad Blodget, Xiaoqi Bao, Mircea Badescu, Yoseph Bar-Cohen

Jet Propulsion Laboratory, California Institute of Technology, 4800 Oak Grove Drive, Pasadena, CA 91109, USA

ABSTRACT

Future NASA missions are increasingly seeking to actuate mechanisms to precision levels in the nanometer range and below. Co-fired multilayer piezoelectric stacks offer the required actuation precision that is needed for such mechanisms. To obtain performance statistics and determine reliability for extended use, sets of commercial PZT stacks were tested in various AC and DC conditions at both nominal and high temperatures and voltages. In order to study the lifetime performance of these stacks, five actuators were driven sinusoidally for up to ten billion cycles. An automated data acquisition system was developed and implemented to monitor each stack's electrical current and voltage waveforms over the life of the test. As part of the monitoring tests, the displacement, impedance, capacitance and leakage current were measured to assess the operation degradation. This paper presents some of the results of this effort.

KEYWORD: piezoelectric devices, positioners, active mirrors, stacks, multilayers

1. INTRODUCTION

A variety of proposed NASA missions including the Space Interferometer Mission (SIM) use precision mechanisms for the control of mirrors surface position. These mechanisms are baselined to use piezoelectric multilayer actuators to achieve the required high precision placement. Controlled movement in the nanometer range is a significant technical challenge. The stability of the actuation mechanism and the ability to sense and control the actuation at this level can be compromised by hysteresis, thermal instability, piezoelectric creep, aging, as well as material property degradation. A variety of manufacturers produce co-fired multilayer actuators and in order to assess the quality and the variance for each supplier 20-30 stacks of similar properties (stroke/volt, capacitance) were procured from four separate suppliers; (Vendor A - PI Ceramic - 30 x P-885.51), (Vendor B - American Piezoelectric Ceramic APC - 30 x 45-1130 Pst150/5x5/20), (Vendor C - Noliac - 25 x Q-JK-20060105-02), and (Vendor D - Sensor Technology - 25 x SJ12-15-0505-00 30). These stacks all have a 5mm x 5 mm nominal cross section. Although a uniform stack length was sought, the stack lengths vary due to vendor availability. (i.e. stacks of length 18mm, 18mm, 20mm, and 15mm were acquired from vendors A, B, C, and D, respectively.) Stacks from vendor A were monolithic co-fired actuators while stacks from the other vendors contained polymer coatings or bond-layers. Further information about these actuators are available in the company catalogs and can be

found according to their part number that is listed above. Screening tests were designed to determine the mean and standard deviation of the elastic, piezoelectric and dielectric properties. The space environment in which these actuators need to operate is nominally benign with respect to temperature and pressure (≈25 ^{o}C, vacuum). However, the inaccessibility after launch and the desired long life operation of the instruments that are driven by these actuation materials (> 5 years preferably 10 years) are a cause of potential concern about their long term performance. In order to determine the life and the level of redundancy required by these mechanisms a lifetime test of five of the actuators for the monolithic co-fired stacks (Vendor A) was executed to assess the degradation and life of these piezoelectric multilayer stacks.

2. Piezoelectric Multilayers

Piezoelectric co-fired stacks or multilayers are used in a variety of applications that require relatively high stress and larger strain than bulk piezoelectric materials can produce. These applications include micro-positioning systems[1] solid state pumps and switches[2], noise isolation mounts[3] and ultrasonic drills and stacked ultrasonic transducers[4]. A variety of papers[5,6,7], have been published on fabrication and characterization of the piezoelectric stack using quasistatic techniques. Figure 1 shows the nominal configuration of a piezoelectric multilayer. The piezoelectric layers are connected mechanically in series and electrically in parallel. The piezoelectric and the electrode materials are placed in a consolidated form and co-fired to produce a monolithic block of material with electrodes that are alternately connected. After co-firing, the stack is poled by raising the temperature closer to the Curie temperature and applying an electric field greater than the coercive field. In some cases, small chips of these co-fired stacks are bonded together to form longer stacks.

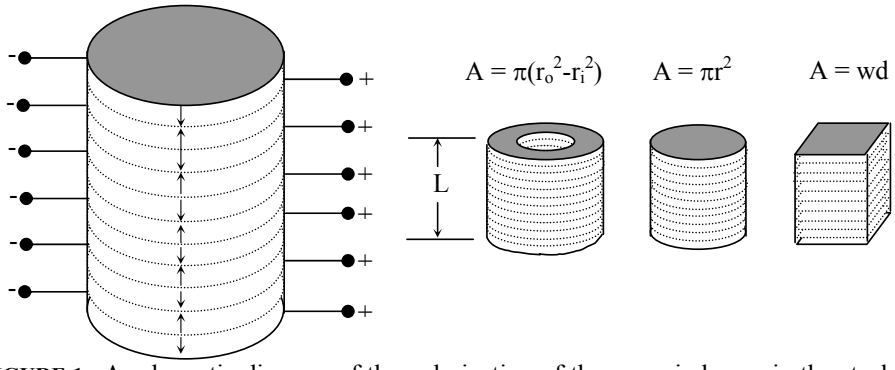

FIGURE 1: A schematic diagram of the polarization of the ceramic layers in the stack and the polarity of the applied signal. The thickness of the piezoelectric is t_P and the thickness of the bond layer is t_b. The figure to the right shows a variety of possible stack cross sections.

3. Screening tests

In the quasistatic limit and assuming zero bond length t_b=0, the effective density of the piezoelectric stack is ρ, the piezoelectric material density, and the effective elastic constant is the Youngs modulus of the poled piezoelectric ceramic material.

The effective piezoelectric constant is determined by summing the displacement for each element of thickness t_p of the stack and is found to be.

$$d_{33eff} = nd_{33\,piezo} \tag{1}$$

Field Code Changed

Where n is the number of layers and d_{33eff} and $d_{33piezo}$ are the effective piezoelectric strain coefficient of the total stack treating it as a material of length L and area A having piezoelectric strain coefficient of the material. The effective dielectric constants of the stack, if it is treated as a monolithic rod, is found by noticing that each of the piezoelectric elements are electrically in parallel and the total capacitance is the sum of the capacitance of each element. The effective permittivity is calculated directly from the total capacitance and the geometry of the stack and it is found to be.

$$\varepsilon^{T}_{33eff} = \frac{nL\varepsilon_{33\,piezo}}{t_p} \tag{2}$$

Field Code Changed

It should be noted that the permittivity of the piezoelectric elements $\varepsilon_{33\,piezo}$ does not necessarily correspond to the free permittivity of the piezoelectric material ε^{T}_{33} since the bonding layer may reinforce the piezoelectric in the plane perpendicular to the poling direction. The power dissipated in the piezoelectric under holding DC and under AC voltage excitation is.

$$P_{DC} = \frac{V^2}{R_{DC}} \qquad P_{AC} = \frac{\omega V^2 C}{2}\tan\delta \tag{3}$$

Field Code Changed

With R_{DC} the DC resistance ($R_{DC} = \rho_{DC} L/A$) and C the capacitance ($C = \varepsilon^{T}_{33eff} A/L$) and tanδ the dielectric dissipation. At higher frequencies the stack can be driven into a free resonance and this result may be used to characterize the stack effective material properties (d_{33eff}, ε^{T}_{33eff}, s^{E}_{33eff}, k_{33eff}) [8], [9].In a previous paper[10], we published a method of determining the complex constants for the stack based on the fundamental free resonance. The fundamental resonance has the same resonance structure as the LT resonance equation and by using equations in the IEEE Standard[11] and relating to the circuit parameters from a Butterworth Van Dyke circuit model (C_0, C_1, L_1, R_1) we can determine the properties in Table 1.

The Butterworth Van Dyke circuit parameters were determined using the built in fitting routines of the Agilent 4294 A impedance analyzer and the average dielectric, elastic and piezoelectric data for the 4 vendor lots are shown in Table 2. along with the standard deviation for each sample lot. A Labview computer program was written to automatically control the impedance analyzer and download the impedance-frequency data and BVD parameters and resonance parameters shown in Table 1. to the computer. An example of resonance spectra for a stack from vendor A is shown in Figure 2 along with the fit to the data. The fit is generally quite good around the resonance frequency up to the anti-resonance frequency where there is some deviation in the phase- frequency data. The results of the tests are shown in Table 2. The data clearly shows two vendors with tighter standard deviations from the mean but we caution that this is likely lot dependant. Samples stacks from each lot were selected for dielectric breakdown and temperature dependence studies and Biased Capacitance and Dissipation studies. Examples of the data for Vendor A are shown in Figures 3-5. The dielectric breakdown measurements in Figure 3 show the voltage applied and

current drawn by the actuator as a function of time for 3 different samples. The voltage was ramped in 5 volt steps at 4.5 second intervals and the current and voltage were monitored at a rate of 5.5 samples/sec. The data was collected and saved using a Labview program connected via a GPIB interface to a Keithley Source meter and two Digital Multimeters (DMM's). The program used GPIB interface to command a Keithley 2400 source meter to output a voltage that was then amplified by a TREK 10/10A high voltage amplifier. The output of the amplifier was applied across the series combination of a 200K Ohm resistor and the stack. The voltage drop across the resistor was read with a Keithley 2001 DMM and sent back to the Labview program via the GPIB interface where it was converted to current (V/R=I). A GPIB controlled Keithley 2700 monitored the output voltage of the amplifier. The stack voltage was calculated by subtracting the voltage drop across the resistor from the output voltage of the amplifier. The data shows the onset of breakdown at about 350-550 volts and complete breakdown between 480 and 550 volts. This is typically 3-4 times the rated voltage for these actuators. In some cases after breakdown the samples partially recovered.

The temperature dependence of the stack from Vendor A is shown in Figure 4. An automated program in Labview was used to control the lab oven and perform a resonance scan and analysis at set temperatures using the HP4294A impedance analyzer. The data is typical of PZT with increases in the permittivity, capacitance and d_{33} as the temperature is increased and decreases in the mechanical Q (circuit Q) as the temperature increases. The elastic constant and the coupling are only slightly temperature dependent.

Table 1. Stack effective parameters determined from Butterworth Van Dyke Circuit parameters (C_0, C_1, L_1, R_1). (L =stack length, A =cross sectional area, ρ =density)

Resonance frequency f_s Anti-resonance frequency f_p	$f_s = \frac{1}{2\pi\sqrt{L_1 C_1}} \approx f_r$ $\quad$ $f_p = \frac{1}{2\pi\sqrt{L_1 \frac{C_0 C_1}{C_0 + C_1}}}$
Circuit Q ≈ Mechanical Q	$Q = \frac{1}{R_1}\sqrt{\frac{L_1}{C_1}}$
Coupling coefficient	$\frac{k_{33}^2}{1-k_{33}^2} = \frac{\pi}{2}\frac{f_P}{f_S}\tan\left(\frac{\pi}{2}\frac{f_P - f_S}{f_S}\right)$
Effective elastic constant (m^2/N)	$s^E = \frac{1}{4\rho f_S^2 L^2}$
Effective dielectric permittivity (F/m)	$\varepsilon_{LF} = \frac{L}{A}(C_1 + C_0)$
Effective piezoelectric constant = Stroke/volt (m/V)	$d_{33}^{eff} = \sqrt{k_{33}^2 s^E \varepsilon_{LF}}$

Table 2. Effective dielectric, piezoelectric and elastic constants determined from the fundamental free resonance of the piezoelectric stacks from 4 vendors.

Effective Coefficient	Vendor A N=30	Vendor B N=30	Vendor C N=25	Vendor D N=24*
d_{33} (pm/V)	340	467	313	279
Standard Dev. %	1.8%	3.1%	1.4%	3.0%
ε^{T}_{33mat} (F/m)	1.40E-08	2.49E-08	1.24E-08	1.01E-08
Standard Dev. %	1.9%	5.7%	1.4%	6.0%
s^{E}_{33} (m^2/N)	1.87E-11	1.75E-11	2.06E-11	2.08E-11
Standard Dev. %	0.92%	0.51%	1.2%	5.0%
Capacitance C (F)	1.48E-06	1.63E-06	1.45E-06	6.01E-07
Standard Dev. %	1.7%	5.5%	1.5%	6.2 %
Stroke/volt (m/V) Small signal	9.54E-08	8.41E-08	9.59E-08	5.27E-8
Standard Dev. %	1.9%	3.1%	1.4%	3.1%

- One sample was omitted due to lack of resonance data in the frequency ranged measured

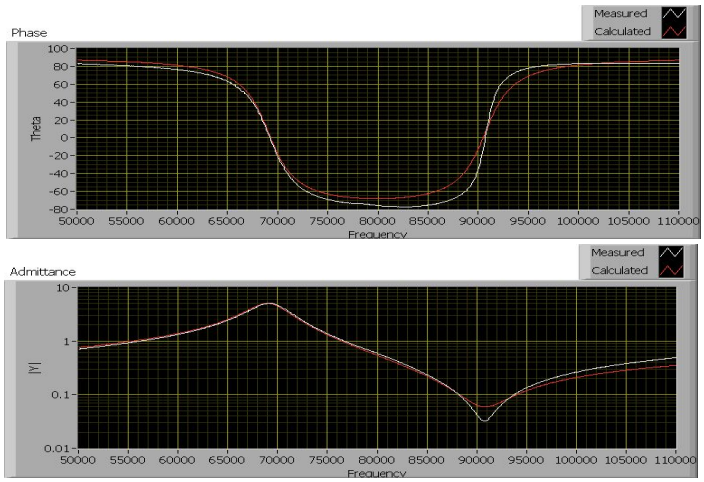

FIGURE 2: Resonance curves - Admittance and Phase (white lines) including BVD circuit fit (red line) to Vendor A stack.

The Capacitance and Dissipation for the stack from Vendor A as a function of the DC bias is shown in Figure 5. Again the data is typical with the Capacitance decreasing slightly with frequency and the dissipation increasing. The DC bias is seen to decrease the capacitance curves while the dissipation curves were found to initially increase with increasing DC bias and then decrease at 20 Volts bias.

4. Lifetime tests

In an effort to determine the lifetime and fatigue behavior under AC operation a test system was designed, built and completed. Since future missions are seeking a long life (> 5 years) and the requirements of each actuator mechanism may vary considerably it becomes impossible to produce a single lifetime test that encompasses

all mechanisms and a choice was made to reduce the scope of the accelerated testing to mimic or at least bound one mechanism which required large stroke.

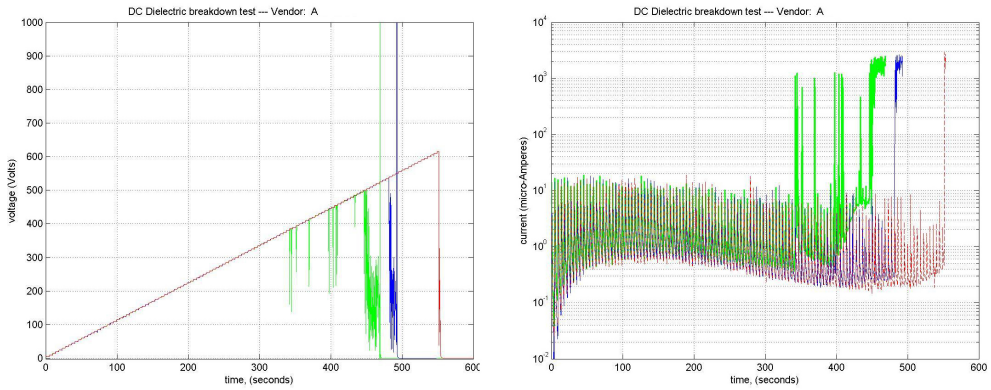

FIGURE 3: Dielectric Breakdown curves for three stacks from Vendor A. The volage (left curve) and current (right curve) as a function of time. The voltage is stepped through 5 volt steps. These particular samples did not show anomalous behavior until reaching 3x to 4x nominal maximum voltage stipulated by the vendor.

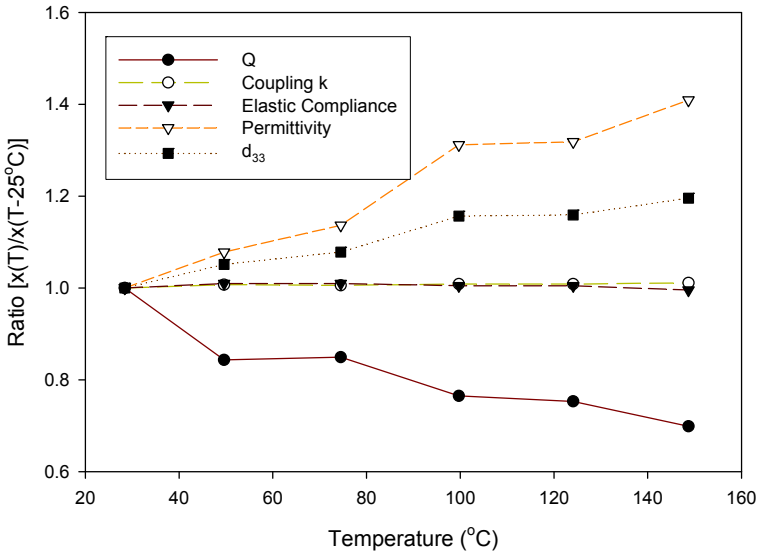

FIGURE 4: Temperature dependence of the effective material properties for a Vendor A stack determined from resonance data.

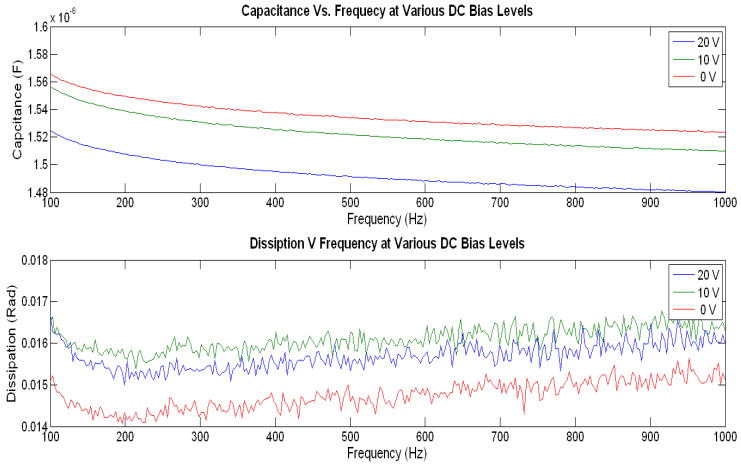

FIGURE 5: Capacitance and Dissipation as a function of frequency for a stack from Vendor A at various DC bias levels

Since this lifetime test did not use flight fixtures and electronics it really is more of a lifetime test of the PZT under certain conditions than a flight related qualification test. These tests therefore are meant as a guide on the performance of PZT stacks and not for any specific mechanism however they do encompass some of the boundary conditions that the actuators are expected to encounter in space operation. In order to accelerate the lifetime test we had to increase the frequency of excitation which also increases the dissipated power and temperature of the actuators however the rise was kept to levels below 55^{o}C. It should be noted that this life test was really a development test where in some instances changes were made at various points in the lifetest to decrease the error. For example the initial 2 billion cycles displayed significant crosstalk in the electrical measurements and methods were devised to reduce this. The fans used for the force convection were also found to fatigue the stack wires at the electrical terminators (not at the stack). In one instance a stack was driven without the forced convection and the generated heat was enough to burnish the electrical buss-bar and melt the solder. It is interesting to note that when the buss-bar was re-soldered the stack returned to nominal values. Much of the initial effort was in designing a suitable test fixture that was reasonably inexpensive to manufacture and met the requirement of the test.

The design requirements of the test fixture were;
a) allow for the removal of the piezoelectric stack,
b) allow for prestressing the stack,
c) allow for the measurement of the stack displacement,
d) allow for the measurement of the prestress level,
e) allow for air flow about the stack,
f) allow for temperature measurement of the stack,
g) had no appreciable resonance in the measurement frequency.

A schematic CAD model and a photograph of the actual test fixture are shown in Figure 6.

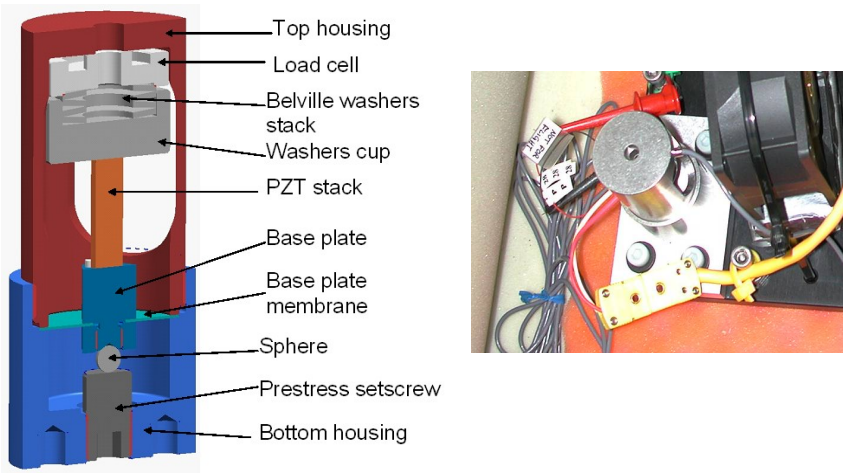

FIGURE 6: CAD model and photograph of the test fixture for lifetime and fatigue testing of the piezoelectric stacks.

The inner surface of the washer cup (shown in Figure 6) was polished to mirror finish so that the stack displacement as a function of voltage can be determined without removing the stack from the assembly. The pre-stress is applied using a set screw through a ball joint to the base-plate of the actuator. The base-plate is rigidized in the plane perpendicular to the actuator extension using a membrane that is clamped and tied between the top and bottom plates. A load cell measures the pre-stress and Bellville washers are used to soften the structure. Ten fixtures were manufactured and instrumented although in this lifetime test we only used 5 actuators and stacks from Vendor A.

The lifetime test was driven at 2000 Hz and 60 Volts between ground and Vpeak. The samples were actively cooled using fans to keep the temperature below a preset limit of 60 ^{o}C. The temperature, voltage, current into the stack including phase information were monitored as a function of the number of cycles. Spot checks including the impedance as a function of frequency, displacement as a function of voltage and the prestress were done at convenient intervals. Figure 7 shows typical displacement curves for one of these actuators as a function of the number of cycles. The displacement was measured using a SIOS interferometer at 1 Hz. The impedance amplitude as a function of the number of cycles is shown in Figure 8. None of the actuators failed during the lifetime test and the number of cycles for the 5 actuators ranged from; 10.6, 10.3, 10.0, 9.6 and 6.8 billion cycles. The 6.8 billion cycle stack was the stack that was overheated (operator error). Changes of the order of 5 to 15% in the impedance values were noted over the course of the lifetest. For example the decrease in the impedance amplitude is of the order of 7% over the course of the lifetest for the stack shown in Figure 8., however, 3% to 5% of this decrease is due to temperature changes over the lifetest. The lifetest was stopped to accommodate another more prolonged test under different conditions and the lessons learned from this lifetest have been incorporated.

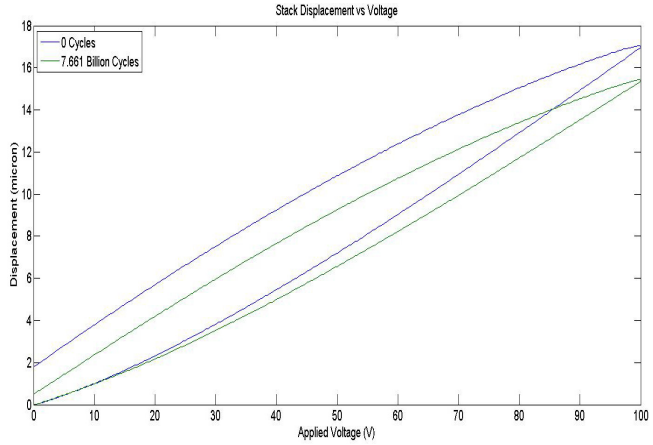

FIGURE 7: The displacement as a function of voltage for a stack from Vendor A after 7.661 billion cycles.

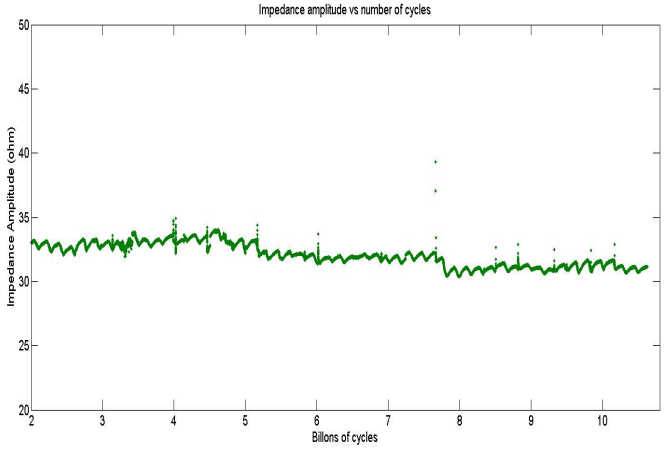

FIGURE 8: An example of **t**he impedance amplitude (V/I) as a function of the number of cycles for a Vendor A stack. The decrease in the impedance amplitude is of the order of 7% over the course of the lifetest.

5. SUMMARY

We reported on the resonance characterization of piezoelectric stack actuators from four vendors. A variety of tests including resonance, DC current, Dielectric Strength, Capacitance and Dissipation were performed to determine the characteristics of the various stacks. In addition temperature studies were also performed to determine the temperature dependence of the stack properties. A lifetime and fatigued tests were completed on a set of stacks up to 10.5 billion cycles. Degradation after 10 billion cycles as determined from the impedance curves is about 7% however a portion of this change (≈3-5%) may be attributed to the change in the

average stack temperature between the start (winter) and finish of the lifetest (spring). A portion of this change is due to change in ambient room temperature and a portion due to increased dissipation during the course of the lifetest.

ACKNOWLEDGMENT

Research reported in this manuscript was conducted at the Jet Propulsion Laboratory (JPL), California Institute of Technology, under a contract with National Aeronautics Space Agency (NASA). The authors would like to thank Jim Moore, John Carson, Paul MacNeal, Dave Braun and Bob Glaser for useful and frank discussions. Reference herein to any specific commercial product, process, or service by trade name, trademark, manufacturer, or otherwise, does not constitute or imply its endorsement by the United States Government or the Jet Propulsion Laboratory, California Institute of Technology.

REFERENCES

[1]Michael Goldfarb, Nikola Celanovic, "Modeling Piezoelectric Stack Actuators for Control of Micromanipulation" , IEEE Control Systems MAG 17: (3) 69-79 JUN 1997

[2] S. Mitsuhashi, K. Wakamatsu, Y. Aihara, N. Okihara, "Relay Using Multilayer Piezoelectric Actuator", Jpn. J. of Appl. Phys. **24** Supp. 24-3, pp. 190-192, 1985

[3] S.A. Wise, M.W. Hooker, Characterization of Multilayer Piezoelectric Actuators for use in Active Isolation Mounts", NASA Langley, NASA Technical Brief - 4742, March, 1997

[4] D.J. Powell, G. Hayward, R.Y. Ting ,"Unidimensional modeling of multi-layered piezoelectric transducer structures", IEEE Trans On Ultrasonics Ferroelectrics and Frequency Control, **45**: (3) pp.667-677, May, 1998

[5] S. M. Pilgrim, A.E. Bailey, M. Massuda, F.C. Poppe, A.P. Ritter, " Fabrication and Characterization of PZT multilayer actuators, Ferroelectrics, **160,** pp. 305-316, 1994

[6] L.S. Bowen, T. Shrout, W.A. Shulze, " Piezoelectric Properties of Internally Electroded PZT Multilayers", Ferroelectrics, **27**, pp.59-62, 1980

[7] B. Zickgraf, G.A. Schneider, F. Aldinger, " Fatigue Behavior of Multilayer Piezoelectric Actuators", Proceedings of the 9th International Symposium on the Applications of Ferroelectrics, University Park, Pennsylvania, pp 325-328, 1994

[8]G.E. Martin, "Vibrations of Coaxially Segmented Longitudinally Polarized Ferroelectric Tubes", JASA **36**, pp. 1496-1506, August 1964.

[9]G.E. Martin, "On the Theory of Segmented Electromechanical Systems" JASA, **36**, pp 1366-1370.

[10]S. Sherrit, S.P. Leary, B.P. Dolgin, Y. Bar-Cohen, R. Tasker, "The Impedance Resonance for Piezoelectric Stacks", Proceedings of the IEEE Ultrasonics Symposium, pp. 1037- 1040, San Juan, Puerto Rico, Oct 22-25, 2000

[11] IEEE Standard on Piezoelectricity IEEE/ANSI Std. 176, 1987